Wind Turbine Gust Load Alleviation Utilizing Curved Blades

Bradley S. Liebst*
University of Minnesota, Minneapolis, Minnesota

The aeroelastic response of curved (i.e., tip sweep in planform) wind turbine blades is analyzed. Numerical results for a 3-bladed, 20-ft radius wind turbine with fiberglass blades were obtained for various tip sweeps. Tip sweeps up to 5 ft appear to provide little tip deflection and bending moment reductions in response to gusts. However, blades with much lower torsional rigidities than the fiberglass blades were shown to provide up to 27% in tip deflections and bending moment relief during gusts.

Nomenclature

a = lift curve slope, $\partial C_L/\partial\alpha$
b = blade elastic axis sweep
b_{tip} = blade sweep at the tip
c = blade chord
C_L = section lift coefficient
C_{MAC} = section moment coefficient
e = distance aerodynamic center is forward of elastic axis
EI = blade flexural rigidity
GJ = blade torsional rigidity
h = hub radius
I_c = blade mass moment of inertia per unit length about the c.g.
I_0 = blade mass moment of inertia per unit length about the elastic axis
L = aerodynamic lift
L = blade curvilinear length
m = blade mass per unit length
M = internal bending moment
M_{Aero} = aerodynamic moment per unit length
M_B = flapwise root bending moment
n = number of blades
N = internal axial force
p = lift per unit length, $dL/d\bar{y}$
q = dynamic pressure, $\frac{1}{2}\rho(\Omega r)^2$
r = radial distance
R = blade radius
s = distance c.g. is forward of the elastic axis
T = internal torsional moment
T_B = root torsional moment
u_d = rotor inflow velocity
$\hat{u}$ = rotor velocity decrement
U_∞ = wind speed
v = distance elastic axis is aft of leading edge
V = internal shear force
V_T = component of relative wind velocity in plane and normal to the elastic axis
w = out of plane elastic axis displacement
w_G = horizontal gust velocity
x,y,z = blade Cartesian axes
$\bar{x},\bar{y},\bar{z}$ = blade curvilinear axes
$\bar{y}$ = direction parallel to the deformed elastic axis
α = local angle of attack
β = angle radial vector makes with the y axis
γ = rotor axis inclination angle
δ = deflection of the trailing edge at the blade tip
η = amplitude of the blade pitch mode
θ = total pitch angle the blade chord makes with the plane of rotation
θ_B = built-in twist angle
θ_E = elastic twist angle
θ_R = root pitch angle
Λ = blade elastic axis slope
ξ = amplitude of the blade bending mode
ρ = air density
σ = local inflow angle
ϕ = assumed bending mode
ψ = assumed torsion mode
Ω = blade rotational speed

Superscripts

$(\dot{})$ = $\partial/\partial t$
$(\,)'$ = $\partial/\partial\bar{y}$

Subscripts

$(\,)_o$ = equilibrium solution

Introduction

MANY wind turbines have their blades upstream of their towers. This configuration is, in fact, preferable over the downstream case where there is blockage of the wind by the tower. One of the disadvantages of placing the blades upstream is the fact that as the blades deflect under the aerodynamic loads, they bend toward the tower. Providing proper clearance for the blades can sometimes be a difficult task. Under high wind conditions a very strong and rapid gust can cause the blades to deflect enough to strike the tower and be destroyed. Active control has been examined for gust load alleviation.[1-3] This, however, would be cost prohibitive for small-scale wind turbines. A possible passive control of this problem might be the utilization of curved blades instead of straight. This is similar to using sweepback in aircraft wings to provide improved aeroelastic properties.[4]

As shown in Figs. 1 and 2 for a curved blade, the outboard sections' aerodynamic centers lie aft of the root section's elastic axis providing a torque. Therefore, a pitching moment at the root results from the internal transmission of these torques. For wind turbines, this pitching moment results in an elastic twist deformation that reduces the angle of attack. Therefore, if a gust occurs resulting in an increase in the aerodynamic force at the aerodynamic centers of each section, this increased force would also result in an elastic twist which acts in such a manner to reduce the aerodynamic loads and, ultimately, to reduce the net blade deflection.

The rest of this paper attempts to demonstrate how effective curved blades would be in providing gust load alleviation. An analysis of curved blades' aeroelastic response is first

Received Sept. 17, 1985; revision received Feb. 3, 1986.

*Assistant Professor, Department of Aerospace Engineering and Mechanics. Senior Member AIAA.

presented; after which, a common small-scale wind turbine with curved blades is evaluated.

Geometry and Mechanical Properties

Several assumptions will be made about the shape and mechanical properties of the tower and rotor. As shown in Fig. 1, the undeformed rotor consists of "banana-shaped" blades whose curvature lies entirely in a plane normal to the axis of rotation. Each blade is sweptback; that is, the convex edge of the blade is the leading edge. The amount of sweep will be defined by the position of the blade's elastic axis, which passes through the shear centers of the blade's cross sections. The airfoil shape may vary along the blade, and there may also be some built-in twist. Pitch changes at the blade root are also possible. Stiffness properties, like flexural and torsional rigidities and mass per length, will be treated as uniform. Elastic, inertia, and aerodynamic forces and moments will be considered to act on (or about) the elastic axis, a line of centers of gravity, and a line of aerodynamic centers, respectively (Fig. 2). The inclined rotor axis is fixed in space, as if the tower was rigid and yaw was prohibited. Each blade will then vibrate independently of the others.

Several coordinate systems will be used in specifying the undeformed blade geometry. All are fixed relative to the blade as it rotates (Fig. 2). The x, y, z system has its origin on the rotor axis, with z positive upwind along that axis. The y direction is radial, intersecting the elastic axis at blade root. $\bar{x}$ and $\bar{y}$ are orthogonal curvilinear coordinates along the elastic axis, with $\bar{y}=0$ at the blade root. Coordinate r is simply the radial distance from the rotor axis. The twist angle of a cross-section is measured between the chordline and its projection on the plane of rotation, positive for leading edge upwind.

Using these coordinates, the position of the elastic axis in the plane of rotation can be defined by the functions $b(y)$, $\Lambda(y)$, or $\beta(y)$, as shown in Fig. 2. Some important relationships between these functions are listed below:

$$\frac{db}{dy}=\tan\Lambda,\quad \frac{b}{y}=\tan\beta,\quad r=\sqrt{y^2+b^2}$$

$$\bar{y}=\int_h^y \sqrt{1+\left[\frac{db}{dy}\right]^2}\,dy$$

Once the elastic axis is specified, the location of the leading edge, the line of aerodynamic centers, and the line of centers of gravity can be described by the functions $v(\bar{y})$, $e(\bar{y})$, and $s(\bar{y})$, respectively. These functions give the distance from the relevant axis to the elastic axis, with positive values in the negative $\bar{x}$ direction.

Blade deformations will be limited to torsion and flapwise bending. Because the blade is curved, coupling will exist between bending and twisting displacements and moments. For example, if a concentrated load is applied to the blade tip parallel to the rotor axis, internal reactions would include both bending and twisting moments. If the blade was loaded such that bending moments are the only internal reaction, the blade would, nevertheless, appear to be twisted because the principal normal vectors for the elastic axis would no longer be parallel to the plane of blade rotation.

For simplicity, most of these coupling effects will be ignored in this analysis. Displacements out of the plane of rotation will be assumed to be caused by bending moments alone and twist will be caused only by twisting moments or by pitching at the root. These approximations will be best when the blade is curved only slightly and pitch changes are small. The only coupling effect to be retained is the interaction of bending and twisting couples in the equations of motion (to be shown later).

The functions $w(\bar{y},t)$ and $\theta_E(\bar{y},t)$ will be used to describe the deflected blade. Here, w is the out of plane component of elastic axis displacement (negative in wind direction), and θ_E is the blade angle elastic rotation due to torsion. Note here that θ_E is only one component of the total angle between the chordline and the plane of rotation. If $\theta(\bar{y},t)$ is the total angle,

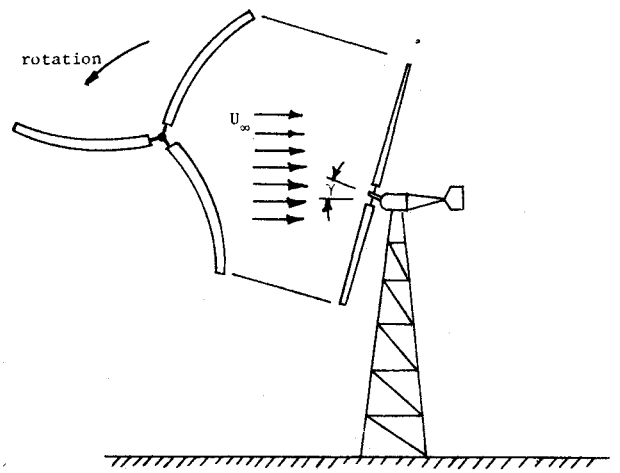

Fig. 1 Wind turbine.

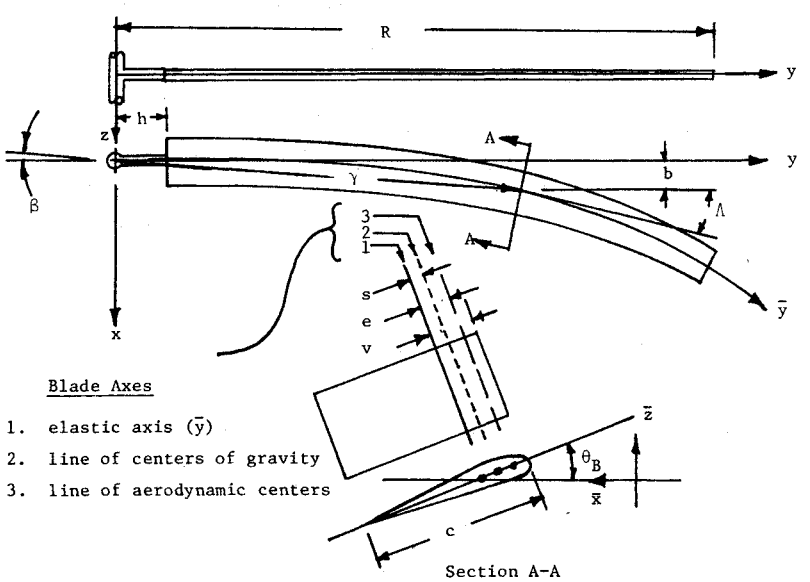

Fig. 2 Blade geometry.

then

$$\theta(\bar{y},t)=\theta_E(\bar{y},t)+\theta_B(\bar{y})+\theta_R(t)$$

Angles θ_B and θ_R are presumed to be given. The functions w and θ_E are unknowns to be determined.

Aerodynamics

A quasisteady aerodynamic analysis will be used. In this analysis, the aerodynamic forces on the blade are calculated as if the instantaneous relative flow velocity was acting steadily. The instantaneous relative wind speed has three sources (Fig. 3): 1) Inflow parallel to the rotor axis $u_d=U_\infty\cos\gamma+w_G(t)\cos\gamma-\hat{u}(\bar{y})$, u_d where $U_\infty\cos\gamma$ is the axial component of average windspeed at tower height, $w_G(t)\cos\gamma$ is the gust velocity component, and $\hat{u}(\bar{y})$ the velocity decrement associated with kinetic energy extraction. 2) blade rotation, Ωr; and 3) blade flapping, $\dot{w}(\bar{y},t)$.

The lift and moment caused by this instantaneous flow velocity will be calculated using aerodynamic properties of two-dimensional airfoils, and drag forces will be ignored. For a blade segment of length $d\bar{y}$, the increments of lift and moment about the aerodynamic center are, respectively,

$$dL=\tfrac{1}{2}\rho V_T^2 c\,d\bar{y}C_L$$

$$dM=\tfrac{1}{2}\rho V_T^2 c^2\,d\bar{y}C_{MAC}$$

For high tip speed ratio, the relative wind speed V_T can be approximated by its component in the plane of rotation, i.e., Ωr. However, the Ωr component does not act normal to the elastic axis. The normal component is $\Omega r\cos(\Lambda-\beta)$, which will be used as V_T. The component of Ωr parallel to the undeformed elastic axis, $\Omega r\sin(\Lambda-\beta)$, will have a small component normal to the deflected elastic axis. The component should be added to the inflow flapping component, i.e., $\dot{w}+\Omega r\sin(\Lambda-\beta)w'$.

Another high tip speed ratio approximation is that the angle σ, between the instantaneous velocity vector and the plane of rotation, is small and can be approximated by its tangent. The local angle of attack can then be written as

$$\alpha=\sigma-\theta=[(U_\infty+w_G)\cos\gamma-\hat{u}+\dot{w}$$

$$+\Omega r\sin(\Lambda-\beta)w'][\Omega r\cos(\Lambda-\beta)]-\theta$$

The axial flow velocity decrement $\hat{u}$ will be found using a modified form of actuator disc theory. Details are given in Ref. 5.

Equations of Motion

Equations of motion will be obtained by considering the dynamic equilibrium of a deformed blade element of length $d\bar{y}$. The direction parallel to the deformed elastic axis will be called $\bar{y}$.

The aerodynamic lift per length $p=dL/d\bar{y}$ acts on the line of aerodynamic centers, perpendicular to the instantaneous relative normal flow vector. The aerodynamic moment per length, M_{Aero}, acts parallel to the deformed elastic axis, and its positive direction is in accordance with the right hand rule.

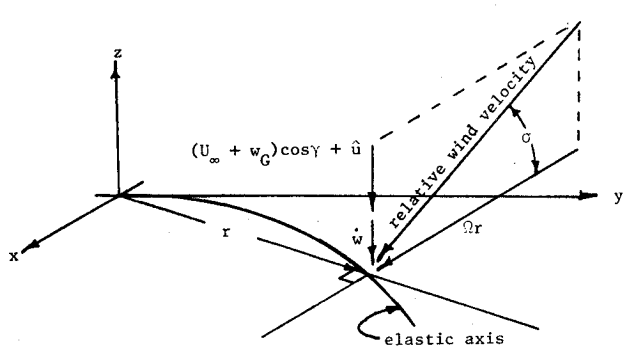

Fig. 3 Relative wind velocity.

Internal reactions are shown in Fig. 4. Twisting couples T and axial forces N act parallel to the deformed elastic axis, while bending moments M act about axes in the local $\bar{x}$ directions. Shear forces V act in the $\bar{y}z$ plane. Because the blade is curved, the directions of any pair of like reactions on opposite faces of the segment may not be parallel, and coupling terms will be introduced into the equations of motion.

The blade element's accelerates normal to the plane of rotation, giving rise to an inertia force per length of $m(\ddot{w}+s\ddot{\theta})$. Another important inertia force is the centrifugal force $m\Omega^2 r$, whose component in the $\bar{z}$ direction is $m\Omega^2 rw'$. This component is the source of centrifugal stiffening. The angular acceleration of the element gives an inertial couple about the c.g. of $I_c\ddot{\theta}$. When moments about the elastic axis are considered, the inertia force in the $\bar{z}$ direction will have a moment of $[m(\ddot{w}+s\ddot{\theta})+m\Omega^2 rw']s$. This inertia couple can also be written as $(I_0-ms^2)\ddot{\theta}$, where I_0 is the mass moment of inertia about the elastic axis. Adding these gives

$$I_0\ddot{\theta}+m\ddot{w}s+mw'\Omega^2 rs$$

which acts in the negative $\bar{y}$ direction. Rotational inertia about other axes will be ignored.

Summing forces and moments about axes fixed to the left face of the blade segment, and setting the sum equal to zero, gives

$$\Sigma F_{\bar{z}}=0=-p+\frac{dV}{d\bar{y}}+Nw''-m(\ddot{w}+s\ddot{\theta})-m\Omega^2 rw' \quad (1)$$

$$\Sigma F_{\bar{y}}=0=\frac{dN}{d\bar{y}}-Vw''+m\Omega^2 r\cos(\Lambda-\beta) \quad (2)$$

$$\Sigma M_x=0=\frac{dM}{d\bar{y}}+T\frac{d\Lambda}{d\bar{y}}+V \quad (3)$$

$$\Sigma M_{\bar{y}}=0=\frac{dT}{d\bar{y}}-M_{Aero}-pe-M\frac{d\Lambda}{d\bar{y}}-I_0\ddot{\theta}-m[\ddot{w}+w'\Omega^2 r]s \quad (4)$$

If bending and torsion are considered to occur independently, the force-deformation equations for a straight beam can be used:

$$M=EIw''$$

$$T=GJ\theta_E'$$

These force-deformation relationships can be placed into Eqs. (3) and (4) to give

$$EIw'''+GJ\theta_e'\Lambda'+V=0 \quad (5)$$

$$GJ\theta_E''-EIw''\Lambda'-M_{Aero}-pe-I_0\ddot{\theta}-ms(\ddot{w}+w'\Omega^2 r)=0 \quad (6)$$

Solving Eq. (5) for V and plugging it into Eqs. (1) and (2), we get

$$-p-[EIw'''+GJ\theta_E'\Lambda']+Nw''-m(\ddot{w}+s\ddot{\theta})-m\Omega^2 rw'=0 \quad (7)$$

$$N'+(EIw'''+GJ\theta_E'\Lambda')w''+m\Omega^2 r\cos(\Lambda-\beta)=0 \quad (8)$$

Equations (6-8) must now be solved for the unknown functions $\theta_E(\bar{y},t)$, $w(\bar{y},t)$, and $N(\bar{y},t)$.

Equilibrium Solution

For $w_G(t)=0$, an equilibrium solution to the blade deflection is determined by setting all d/dt terms to zero

$$-p_o-[EIw_o'''+GJ\theta_{E_o}'\Lambda']'+N_o'w_o''-m\Omega^2rw_o'=0 \quad (9)$$

$$N_o'+(EIw_o'''+GJ\theta_{E_o}'\Lambda')w_o''+m\Omega^2r\cos(\Lambda-\beta)=0 \quad (10)$$

$$GJ\theta_{E_o}'-EIw_o''\Lambda'-M_{\text{Aero}_o}-p_oe-msw_o'\Omega^2r=0 \quad (11)$$

where

$$p_o=\tfrac{1}{2}\rho a[\Omega r\cos(\Omega-\beta)]^2c\alpha_o$$

$$\alpha_o=[U_\infty\cos\gamma-\hat{u}+\Omega r\sin(\Lambda-\beta)w_o'/\Omega r\cos(\Lambda-\beta)]-\theta_{E_o}-\theta_B-\theta_R$$

$$M_{\text{Aero}_o}=\tfrac{1}{2}\rho[\Omega r\cos(\Lambda-\beta)]^2c^2C_{\text{MAC}}$$

Gust Response

To obtain the gust response, the equations of motion will be solved approximately with an assumed mode solution of the form

$$w(\bar{y},t)=w_o(\bar{y})+\phi(\bar{y})\xi(t)$$

$$\theta_E(\bar{y},t)=\theta_{E_o}(\bar{y})+\psi(\bar{y})\eta(t)$$

where ϕ and ψ are, respectively, the fundamental bending and torsion modes of a straight cantilevered blade of constant cross-sectional properties, and their amplitudes ξ and η are assumed small. Thus,

$$\phi(\bar{y})=\sin[(K_1/L)\bar{y}]-\sinh[(K_1/L)\bar{y}]+K_2\{\cosh[(K_1/L)\bar{y}]-\cos[(K_1/L)\bar{y}]\}$$

$$\psi(\bar{y})=\sin[(K_3/L)\bar{y}]$$

where

$$K_1=1.875, \qquad K_2=1.362, \qquad K_3=1.571$$

Inserting these assumed solutions into Eqs. (6) and (7), while neglecting both N and higher order perturbations and cancelling out the equilibrium solutions yields

$$EI\Lambda'\phi''\xi-GJ\psi''\eta+I_0\psi\ddot{\eta}+ms\phi\ddot{\xi}+ms\Omega^2r\phi'\xi+\tfrac{1}{2}\rho ae[\Omega r\cos(\Lambda-\beta)]c\phi\dot{\xi}-\tfrac{1}{2}\rho ae[\Omega r\cos(\Lambda-\beta)]^2c\psi\eta=-\tfrac{1}{2}\rho ae[\Omega r\cos(\Lambda-\beta)]c\cos\gamma w_G \quad (12)$$

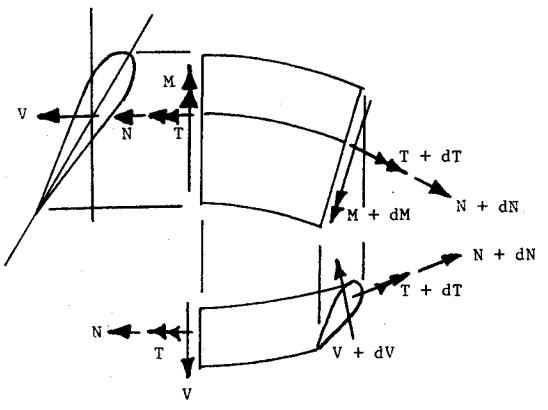

Fig. 4 Internal reactions.

and

$$EI\phi''''\xi+GJ\Lambda'\psi''\eta+GJ\Lambda''\psi'\eta-N_o\phi''\xi+m\phi\ddot{\xi}+ms\psi\ddot{\eta}+m\Omega^2r\phi'\xi-\tfrac{1}{2}\rho a[\Omega r\cos(\Lambda-\beta)]^2c\psi\eta+\tfrac{1}{2}\rho a[\Omega r\cos(\Lambda-\beta)]c\phi\dot{\xi}=-\tfrac{1}{2}\rho a[\Omega r\cos(\Lambda-\beta)]c\cos\gamma w_G \quad (13)$$

Multiplying Eq. (12) by ψ and Eq. (13) by ϕ, and integrating from $\bar{y}=0$ into $\bar{y}=L$, gives the following linear second order system:

$$\begin{bmatrix}m_{11} & m_{12}\\ m_{21} & m_{22}\end{bmatrix}\begin{bmatrix}\ddot{\xi}\\ \ddot{\eta}\end{bmatrix}+\begin{bmatrix}b_{11} & b_{12}\\ b_{21} & b_{22}\end{bmatrix}\begin{bmatrix}\dot{\xi}\\ \dot{\eta}\end{bmatrix}+\begin{bmatrix}k_{11} & k_{12}\\ k_{21} & k_{22}\end{bmatrix}\begin{bmatrix}\xi\\ \eta\end{bmatrix}=\begin{bmatrix}Q_1\\ Q_2\end{bmatrix}w_G(t) \quad (14)$$

The coefficients for the above matrices are listed in the Appendix.

The linear system, Eq. (14), can be solved numerically to yield a time history for $\xi(t)$ and $\eta(t)$. Once these are known, the blade tip deflection and root flapwise bending and torsional moments can be calculated. If δ is the deflection at the trailing edge of the tip (positive in the wind direction),

$$\delta=-w(L,t)+(c-v)(\theta_E(L,t)+\theta_B(L)+\theta_R)$$
$$=-w_o(L)-\phi(L)\xi(t)+(c-v)[\theta_{E_o}(L)+\psi(L)\eta(t)+\theta_B(L)+\theta_R]$$
$$=-2.723\xi(t)+(c-v)\eta(t)-w_o(L)+(c-v)[\theta_{E_o}(L)+\theta_B(L)+\theta_R] \quad (15)$$

The flapwise bending moment at the root is

$$M_B=EIw''(0,t)=EI(w_o''(0)+\phi''(0)\xi(t))$$
$$=EIw_o''(0)+9.577\,(EI/L^2)\xi(t) \quad (16)$$

The root torsional moment is

$$T_B=GJ\theta_E'(0,t)=GJ[\theta_{E_o}'(0)+\psi'(0)\eta(t)]$$
$$=GJ\theta_{E_o}'(0)+(1.571/L)GJ\eta(t) \quad (17)$$

Table 1 Wind turbine data

Number of blades, N	3
Blade chord, c, ft	.5
Blade radius, R, ft	20
Blade material	fiberglass
Air density, ρ, slug/ft^3	.00238
Rotational velocity, Ω, rpm	130
Lift curve slope, a	6
Moment coefficient, C_{MAC}	0
Steady-state windspeed, U_∞, mph	20
Rotor axis inclination, γ, deg	0
Hub radius, h, ft	.75
Mass per unit length, m, slug/ft	.112
Moment of inertia per length, I_0, slug-ft	.0018
Distance to aerodynamic center, e, ft	0
Distance to c.g., s, ft	0
Distance elastic axis is aft of the leading edge, v, ft	.125
Flexural rigidity, EI, lb-ft^2	28512
Torsional rigidity, GJ^*, lb-ft^2	21384
Steady-state power, kW	10
Blade twist, θ_B, deg	0

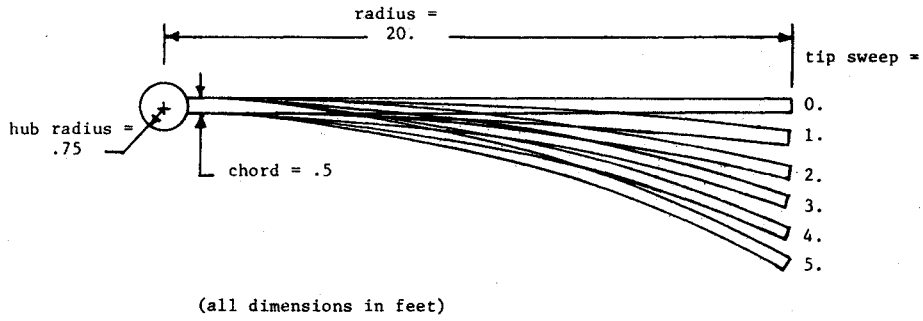

Fig. 5 Swept blade planforms.

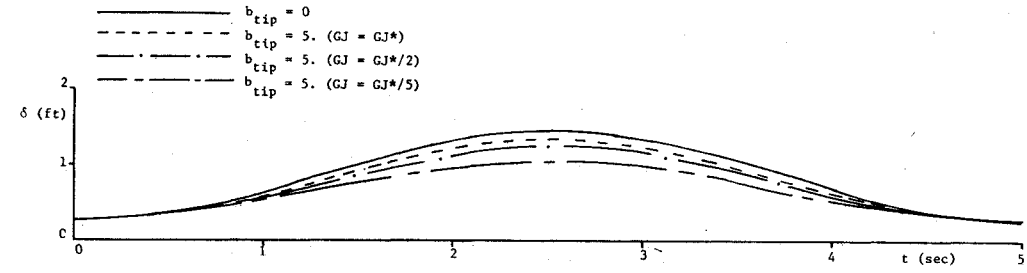

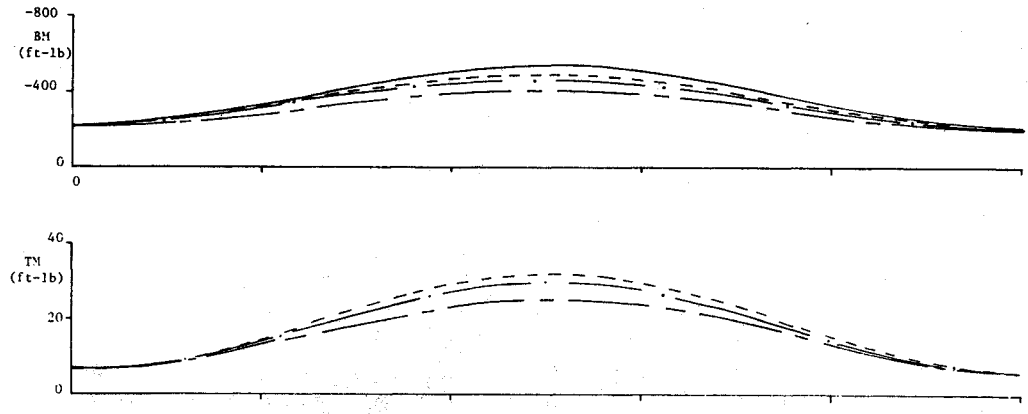

Fig. 6 Wind turbine response to a 5.0 s, 20 mph gust.

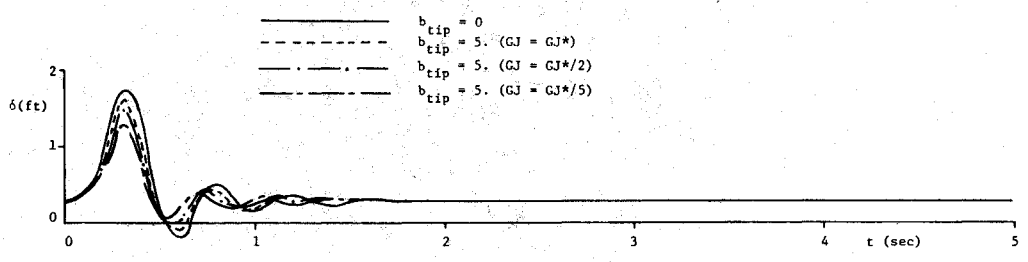

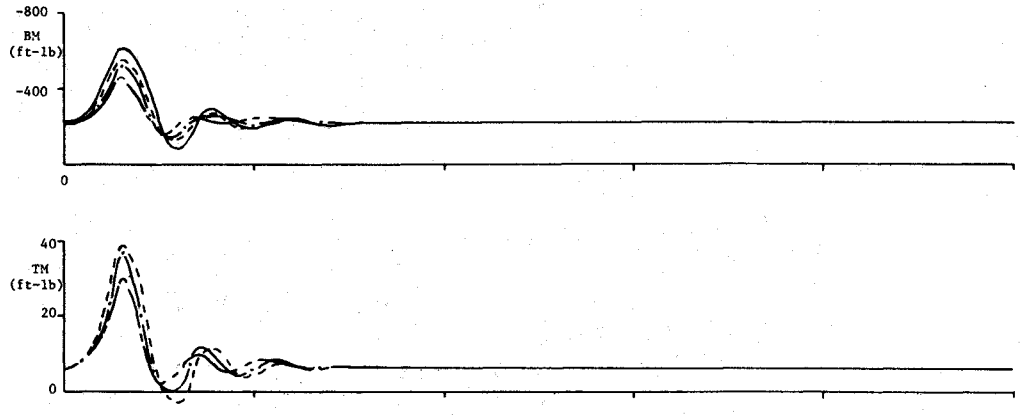

Fig. 7 Wind turbine response to a 0.5 s, 20 mph gust.

Table 2 Wind turbine response due to two gusts with $GJ = GJ^*$

	Maximum tip deflection, ft		Maximum root bending moment, ft-lb		Maximum root torsional moment, ft-lb	
Tip sweep, ft	$t_g = 5.0$	$t_g = 0.5$	$t_g = 5.0$	$t_g = 0.5$	$t_g = 5.0$	$t_g = 0.5$
0	1.44	1.74	538.0	619.0	0.0	0.0
1	1.41	1.71	529.0	609.0	7.3	8.8
2	1.39	1.68	516.0	596.0	14.0	17.1
3	1.37	1.67	506.0	584.0	20.5	25.0
4	1.35	1.65	492.0	568.0	26.4	32.2
5	1.34	1.64	482.0	556.0	31.9	39.0

Table 3 Wind turbine response due to two gusts with $GJ = GJ^*/2$

	Maximum tip deflection, ft		Maximum root bending moment, ft-lb		Maximum root torsional moment, ft-lb	
Tip sweep, ft	$t_g = 5.0$	$t_g = 0.5$	$t_g = 5.0$	$t_g = 0.5$	$t_g = 5.0$	$t_g = 0.5$
0	1.44	1.74	538.0	619.0	0.0	0.0
1	1.39	1.69	524.0	604.0	7.2	8.7
2	1.35	1.64	506.0	584.0	13.7	16.7
3	1.31	1.60	491.0	568.0	19.7	24.7
4	1.28	1.57	475.0	549.0	25.0	30.7
5	1.25	1.54	461.0	531.0	29.9	36.7

Table 4 Wind turbine response due to two gusts with $GJ = GJ^*/5$

	Maximum tip deflection, ft		Maximum root bending moment, ft-lb		Maximum root torsional moment, ft-lb	
Tip sweep, ft	$t_g = 5.0$	$t_g = 0.5$	$t_g = 5.0$	$t_g = 0.5$	$t_g = 5.0$	$t_g = 0.5$
0	1.44	1.74	538.0	619.0	0.0	0.0
1	1.33	1.63	508.0	587.0	6.9	8.4
2	1.24	1.52	479.0	553.0	12.7	15.6
3	1.17	1.44	457.0	526.0	17.8	21.8
4	1.11	1.36	434.0	495.0	22.0	26.8
5	1.05	1.27	408.0	462.0	25.0	30.3

Numerical Example

To determine the effectiveness of curved blades, a typical small-scale three-bladed wind turbine with fiberglass blades was chosen for evaluation. The values for the wind turbine parameters are given in Table 1. This fictitious wind turbine has very similar characteristics to many of the small-scale wind turbines currently on the market. The blade curvature chosen for the present study was parabolic:

$$b(y) = (b_{\text{tip}}/R^2)y^2 \tag{18}$$

Thus,

$$\Lambda(y) = \tan^{-1}[(2b_{\text{tip}}/R^2)y] \tag{19}$$

$$\beta(y) = \tan^{-1}[(b_{\text{tip}}/R^2)y] \tag{20}$$

$$r = y\sqrt{1 + [(b_{\text{tip}}/R^2)y]^2} \tag{21}$$

$$\bar{y} = [(b_{\text{tip}}/R^2]\left[y\sqrt{[(R^2/2b_{\text{tip}})]^2 + y^2} - h\sqrt{[R^2/2b_{\text{tip}})]^2 + h^2}\right.$$
$$\left. + [(R^2/2b_{\text{tip}})]^2 \ell n\left[\frac{y + \sqrt{[(R^2/2b_{\text{tip}})]^2 + y^2}}{h + \sqrt{[(R^2/2b_{\text{tip}})]^2 + h^2}}\right]\right] \tag{22}$$

Tip sweep values of 0, 1, 2, 3, 4, and 5 ft were all examined. A plot of these planforms is shown in Fig. 5.

To determine the gust responses reported in Tables 2 and 4 and Figs. 6 and 7 the following procedures were applied.

1) The equilibrium solutions were first obtained by solving the nonlinear differential Eqs. (9-11) by a shooting method with cantilever beam boundary conditions. The root pitch was varied until the steady-state output power was 10 kW in each case.

2) The coefficients of the linear differential Eq. (14) are then calculated with the steady-state values previously determined.

3) The solutions to the gust response were found by Runge-Kutta numerical solution of Eq. (14) for a NASA standard 1-cosine gust[6] input of 20 mph amplitude.

4) With $\xi(t)$ and $\eta(t)$ determined the tip deflection, root bending moment, and root torsional moment responses can be determined from Eqs. (15-17).

Two different gust duration times were examined: a relatively slow gust of 5.0 s duration and a relatively fast gust of 0.5 s duration. The wind turbine response to the 5.0 s gust is shown in Fig. 6 and the response to the 0.5 s gust is shown in Fig. 7. The solid line is the straight blade ($b_{\text{tip}} = 0$) and the dashed line is for a blade tip sweep of 5.0 ft and the nominal torsional rigidity ($GJ^* = 21384$ lb-ft^2). The values of the maximum tip deflection, root bending moment, and root torsional moment for each gust duration at various tip sweep values are tabulated in Table 2 for the nominal torsional rigidity.

With maximum tip deflections of the order of 2 ft or less and a 20 ft blade radius, the small deflection assumption appears to be valid. In Fig. 7, it can be seen that the blade is responding to the gust pulse by ringing at its bending natural frequency. Table 2 shows that very little tip deflection and root loading relief is provided by the curved blades. Even with

the 5.0 ft sweep, there is only a 7% reduction in maximum tip deflection in the 5.0 s gust and a 6% reduction in the 0.5 s gust case. These are certainly not very impressive considering the added expenses that would be incurred in producing curved blades as opposed to straight blades. An additional penalty to be paid in an increased torsional moments. The stresses induced for the present case are nothing significant but might be for greater sweeps.

To obtain further reductions in blade response one must achieve greater elastic pitch reductions. This can certainly be done by reducing torsional rigidity as well as increasing tip sweep. Table 3 is the response of an identical turbine to that of Table 2 except with a torsional rigidity one-half that of the nominal. Table 4 is for a turbine with a torsional rigidity one-fifth that of the nominal. Figure 6 and 7 also include the time histories of the gust responses for these two cases as well. Reductions up to 27% in blade response are shown. This is somewhat impressive but unrealistic since changing the material to reduce the torsional rigidity in half would do approximately the same to the flexural rigidity resulting in proportionally greater tip deflections.

Conclusions and Recommendations

It is apparent from the numerical example that typical small-scale wind turbines would benefit only slightly from curved blades. For the 20-ft fiberglass blades examined, tip deflection reduction and flap bending moment relief on the order of 6 to 7% were obtained for a 5 ft tip sweep. This is hardly justification for the added expense and complexity incurred in producing curved blades. The 27% reduction obtained with blades of much reduced torsional rigidity are very encouraging, however. They indicate that low torsional and high flexural rigidities are necessary for the curved blades to be effective.

Aeroelastic tailoring with composite materials of the blades to independently vary the flexural and torsional rigidities would likely be cost prohibitive. A simplier, more cost effective solution would be to connect curved blades to the hub by flexible torsional springs. This arrangement would allow for the aerodynamic angle of attack relief necessary without the need for low torsional rigidity and large elastic twist deformations.

It is believed that the concept of curved blades connected to root springs may have promise. This combination should be investigated to determine the root spring requirements which achieve significant gust load alleviation, as well as whether or not it is practical from the construction standpoint.

Appendix

Coefficients of the mass, damping, and stiffness matrices are

$$m_{11}=\int_0^L m\phi^2 d\bar{y}, \qquad m_{12}=\int_0^L ms\psi\phi d\bar{y}$$

$$m_{21}=m_{12}, \qquad m_{22}=\int_0^L I_o\psi^2 d\bar{y}$$

$$b_{11}=\int_0^L \frac{q\cos(\Lambda-\beta)ca\phi^2}{\Omega r}d\bar{y}, \qquad b_{12}=0$$

$$b_{21}=\int_0^L \frac{q\cos(\Lambda-\beta)ca e\phi\psi}{\Omega r}d\bar{y}, \qquad b_{22}=0$$

$$k_{11}=\int_0^L \phi[EI\phi'''' - N_o\phi'' + m\Omega^2 r\phi']d\bar{y}$$

$$k_{12}=\int_0^L \phi[GJ\Lambda'\psi'' + GJ\Lambda''\psi' - q\cos^2(\Lambda-\beta)ca\psi]d\bar{y}$$

$$k_{21}=\int_0^L \psi[EI\phi''\Lambda' + ms\phi'\Omega^2 r]d\bar{y}$$

$$k_{22}=\int_0^L \psi[-GJ\psi'' - q\cos^2(\Lambda-\beta)ca e\psi]d\bar{y}$$

$$Q_1=\int_0^L \frac{-\phi q\cos(\Lambda-\beta)ca\cos\gamma}{\Omega r}d\bar{y}$$

$$Q_2=\int_0^L \frac{-\psi q\cos(\Lambda-\beta)ca e\cos\gamma}{\Omega r}d\bar{y}$$

where $q=\frac{1}{2}\rho(\Omega r)^2$.

References

[1]Liebst, B. S., "A Pitch Control System for Large Scale Wind Turbines," *Journal of Energy*, Vol. 3, May-June, 1983, pp. 182-192.

[2]Liebst, B. S., "A Pitch Control System for the KaMeWa Wind Turbine," *Journal of Dynamic Systems, Measurement and Control*, Vol. 3, May-June 1985, pp. 47-52.

[3]Hinrichsen, E. N., "Controls for Variable Pitch Wind Turbine Generators," *IEEE Transactions on Power Apparatus and Systems*, Vol. 3, April, 1984, pp. 886-892.

[4]Bisplinghoff, R., Ashley, H., and Halfman, R., *Aeroelasticity*, Addison-Wesley Publishing Co., Reading, MA, 1955, pp. 474-516.

[5]Miller, R. H. et al., "Wind Energy Conversion," Vol. I-X, Department of Energy Rept. COO-4131-TI, 1980.

[6]Liebst, B. S., "A Pitch Control System for Large Scale Wind Turbines," FFA, The Aeronautical Research Institute of Sweden, Tech. Note HU-2262, Pt. 6, 1981, pp. 104-105.